

New thorium and uranium monophosphates in the $KTh_2(PO_4)_3$ family: structure and cationic non-stoichiometry

Anne Guesdon,* Jackie Provost and Bernard Raveau

Laboratoire CRISMAT, UMR 6508 associée au CNRS, ISMRA et Université de Caen, 6, Boulevard du Maréchal Juin, 14050 Caen Cedex, France.

E-mail: anne.guesdon@ismra.fr

Received 24th May 1999, Accepted 14th July 1999

A new uranium monophosphate $KU_2(PO_4)_3$ has been synthesized. The structure of this phase, isotypic with $KTh_2(PO_4)_3$, has been determined using a single crystal. The analysis of this structure leads to a new description, in which the $[U_2(PO_4)_3]_\infty$ framework, built up of edge- and corner-sharing PO_4 tetrahedra and UO_6 polyhedra, forms eight-sided tunnels. New non-stoichiometric phosphates, $A_{0.5}Th_2(PO_4)_3$ with $A = Ba, Sr, Pb, Ca, Cd$ and $K_{1-2x}Ba_xTh_2(PO_4)_3$, have been synthesized, showing the great flexibility of this structure.

Introduction

Taking into account the ability of several natural inorganic compounds to accept actinide elements in their structure, combined with their great stability, the use of crystalline phases as storage materials for nuclear waste has recently been suggested as a possible alternative to glass matrices. More particularly, phosphates appear to be good candidates since they can form very resistant structures with thorium or uranium (see for example the series of monazite structure type compounds¹). However, the number of these inorganic actinide phosphates known up to now²⁻¹⁴ is rather small compared with other phosphate compounds. Among these materials, the thorium monophosphates $A^I Th_2(PO_4)_3$ form a large family with $A = K, Rb, Cs, Tl, Cu, Ag, Na$,⁸⁻¹⁴ showing the ability of the $Th_2(PO_4)_3$ framework to host various cations. Tetravalent uranium chemistry seems to be less well studied, in spite of its great similarity with thorium. Only two isostructural uranium monophosphates $A^I U_2(PO_4)_3$ have been synthesized to date, with $A = Na, Li$,^{8,9} but no single crystal structure determination has been performed for the latter. In order to understand this behavior we have thus reinvestigated the $A^I M_2(PO_4)_3$ family with $M = U, Th$. We report herein the synthesis and crystal structure of a series of new monophosphates, $KU_2(PO_4)_3$ and $A_{0.5}Th_2(PO_4)_3$ with $A = Ba, Sr, Pb, Ca, Cd$, and we discuss the cationic non-stoichiometry in these compounds, on the basis of the $M_2(PO_4)_3$ host lattice. The magnetic properties of the uranium phases have also been investigated.

Experimental

Synthesis and crystal growth

The synthesis of $KM_2(PO_4)_3$, $A_{0.5}M_2(PO_4)_3$ with $A = Ba, Sr, Pb, Ca, Cd$ and $Ba_xK_{1-2x}Th_2(PO_4)_3$ monophosphates, with $M = Th, U$, was carried out in two steps. In the first step, intimate mixtures of ACO_3 and/or A_2CO_3 , $PO_4H(NH_4)_2$ and ThO_2 or UO_2 were heated in platinum crucibles in air at 673 K in order to decompose the carbonates and the ammonium phosphate. Note that at this temperature UO_2 is not oxidized. In the second step the thorium phosphates were heated in air in a platinum crucible at 1473 K for 12 h, whereas the uranium phosphates were heated at temperatures ranging from 1173 to 1323 K for 12 h in an evacuated silica ampoule in order to avoid oxidization of U(IV). Attempts were also made to

synthesize the uranium phosphates *via* an alternative route: mixtures of ACO_3 and/or A_2CO_3 and $PO_4H(NH_4)_2$ were first heated in air at 673 K, then the resulting compounds were added to UO_2 and heated in evacuated ampoules at the same temperatures as above, ranging from 1173 to 1323 K. The products were identical to those obtained from the first method.

The single crystal used for the structure determination of $KU_2(PO_4)_3$ was grown from a mixture of nominal composition $K_4U_3P_3O_{17}$, synthesized in two steps: first K_2CO_3 , $(NO_3)_2UO_2 \cdot 6H_2O$ and $PO_4H(NH_4)_2$ were mixed in an agate mortar, placed in a platinum crucible and heated in air at 673 K in order to decompose the potassium carbonate, the uranyl nitrate and the ammonium phosphate. The appropriate amount of UO_2 was then added and the resulting mixture was sealed in an evacuated silica ampoule. This was heated at 1373 K for 20 h and then cooled at a rate of $15 K h^{-1}$ down to 298 K. Green crystals of the desired product were extracted from the resulting mixture. Their EDS analyses, performed with a Tracor microprobe mounted on a JEOL 840 scanning electron microscope, led to the approximate cationic composition KU_2P_3 , which was confirmed by the structure determination.

X-Ray diffraction study and EDS analyses

The X-ray powder diffraction data were collected with a Philips diffractometer using $Cu-K\alpha$ radiation ($\lambda = 1.5406 \text{ \AA}$) in steps of 0.02° in 2θ within the angular ranges $5^\circ \leq 2\theta \leq 80^\circ$ for $KU_2(PO_4)_3$ and $KUTh(PO_4)_3$ and $5^\circ \leq 2\theta \leq 100^\circ$ for all the other compounds. The cell parameters were refined using the Fullprof program.¹⁵ Cationic compositions were checked by means of transmission electron microscopy (TEM), performed with a JEOL 200CX microscope equipped with a eucentric goniometer ($\pm 60^\circ$) and EDS analysers.

A single crystal study was performed on $KU_2(PO_4)_3$. Several green parallelepiped shaped crystals of $KU_2(PO_4)_3$ were selected optically and tested by the oscillation and Weissenberg methods using $Cu-K\alpha$ radiation. A single crystal with dimensions of $0.051 \times 0.039 \times 0.026 \text{ mm}$ was chosen for the structure determination. The cell parameters, reported in Table 1, were determined and refined by diffractometric techniques at 293 K using a least squares method based upon 25 reflections in the range $18^\circ < \theta < 22^\circ$. The data were collected on a CAD4 Enraf-Nonius diffractometer using $Mo-K\alpha$ radiation ($\lambda = 0.71073 \text{ \AA}$). The reflections were corrected

Table 1 Summary of crystal data, intensity measurements and structural refinement parameters for $\text{KU}_2(\text{PO}_4)_3$

Chemical formula	$\text{KU}_2(\text{PO}_4)_3$
Formula weight/ g mol^{-1}	800.07
Crystal system	Monoclinic
Space group	$C2/c$ (no. 15)
μ/mm^{-1}	35.95
R values	$R=0.038$, $R_w=0.036$
Unit cell dimensions	$a=17.479(2)$ Å $b=6.758(1)$ Å, $\beta=102.01(1)^\circ$ $c=8.019(1)$ Å
Unit cell volume/Å ³	926.5(3)
Temperature/K	293
Z	4
Measured reflections	4190
Reflections with $I > 3\sigma$	1740
Parameters refined	89

for Lorentz and polarization effects, and for absorption and secondary extinction. The Laue symmetry is m and the systematic absences $h+k=2n+1$ for hkl and $l=2n+1$ for $h0l$ are consistent with the space groups Cc and $C2/c$. However, the Patterson function presents a Harker plane ($u0w$) that corresponds to the existence of two-fold axes and indicates that the space group is $C2/c$. The structure was thus solved in this centrosymmetric space group, with the heavy atom method. The refinement of the atomic coordinates and of the anisotropic thermal factors of all atoms led to $R=0.038$ and $R_w=0.036$ and to the atomic parameters listed in Table 2. Note that the potassium atom was at first placed on the two-fold axis, but the refinement led to a rather high value for its thermal factor ($U_{\text{eq}}=0.075$ Å²). Moreover, examination of the Fourier difference map showed residual electron density close to the position of the potassium atom although it was refined anisotropically. The potassium atom was thus situated out of the two-fold axis; the refinement of its position and of its anisotropic thermal factors then led to an equivalent thermal parameter of 0.03 Å² and the final difference Fourier map no longer showed any electronic residue around the position of the K atom. The calculations were performed on a SPARK station with the XTAL 3.2 package.¹⁶

Full crystallographic details, excluding structure factor tables have been deposited at the Cambridge Crystallographic Data Centre (CCDC). For details of the deposition scheme, see 'Information for Authors', *J. Mater. Chem.*, available via the RSC web site (<http://www.rsc.org/authors>). Any request to the CCDC for this material should quote the full literature citation and the reference number 1145/173. See <http://www.rsc.org/suppdata/jm/1999/2583> for crystallographic files in .cif format.

Table 2 Positional parameters and their estimated standard deviations in $\text{KU}_2(\text{PO}_4)_3$

Atom	x	y	z	$100 U_{\text{eq}}/\text{Å}^2$
K	-0.0083(7)	0.4006(9)	0.212(1)	3.3(3)
U	0.15385(2)	0.09374(6)	0.03463(5)	0.710(7)
P(1)	1/2	0.4011(8)	1/4	0.94(9)
P(2)	0.3099(1)	0.896(6)	0.3175(3)	0.81(6)
O(1)	0.2242(4)	0.049(1)	0.3310(9)	0.9(2)
O(2)	0.0726(4)	0.033(1)	0.2448(9)	1.2(2)
O(3)	0.0270(4)	0.220(1)	-0.087(1)	1.4(2)
O(4)	0.1536(4)	-0.241(1)	0.0687(8)	1.0(2)
O(5)	0.2977(4)	0.154(1)	0.1276(9)	1.1(2)
O(6)	0.1413(3)	0.402(1)	0.1540(9)	1.3(2)

All atoms were refined anisotropically and are given in the form of the isotropic equivalent displacement parameter, defined as:

$$U_{\text{eq}} = \frac{1}{3} \sum_{i=1}^3 \sum_{j=1}^3 U^{ij} a_i a_j$$

Refinement of the site occupation for the potassium atom led to the value of 0.501(8).

Magnetic characterization

Magnetic susceptibility measurements were performed on powder samples of $\text{KU}_2(\text{PO}_4)_3$ and $\text{KTh}(\text{PO}_4)_3$ by SQUID magnetometry. After zero cooling and stabilization of the temperature at 4.5 K, a magnetic field of 0.3 T was applied. The magnetic moments were then measured with increasing temperature up to 300 K. The magnetic signal of the sample holder, measured in the same conditions, was subtracted from the total measured moments.

Results and discussion

Under the above experimental conditions a new uranium monophosphate, $\text{KU}_2(\text{PO}_4)_3$, was synthesized as a pure phase whose XRPD pattern was indexed in a monoclinic cell with parameters similar to those obtained for the $\text{KTh}_2(\text{PO}_4)_3$ -type structure (Table 1). Single crystals of this phase were grown for a structural study. The analysis of the structure of this phase led us to a new description, showing that the PO_4 tetrahedra and UO_9 polyhedra form a tunnel structure where K^+ cations are interpolated. Based on this description, the possibility of cationic non-stoichiometry in the $\text{KTh}_2(\text{PO}_4)_3$ -type structure was investigated in a second step.

Description of the structure of $\text{KU}_2(\text{PO}_4)_3$

The atomic parameters of this phase obtained after refinement (Table 2) confirm that it is isotypic with $\text{KTh}_2(\text{PO}_4)_3$.¹⁰ The projection of the structure along c (Fig. 1) shows that it is indeed built from PO_4 monophosphate groups and UO_9 polyhedra, similar to the ThO_9 polyhedra, sharing their apices and their edges.

The important feature of this structure concerns the three dimensional character of the $[\text{U}_2(\text{PO}_4)_3]_\infty$ framework. The projection of the structure along b (Fig. 2) shows that the $[\text{U}_2(\text{PO}_4)_3]_\infty$ framework consists of the stacking along a of $[\text{U}_2\text{O}_6\{\text{P}(2)\text{O}_4\}_2]_\infty$ double layers connected through $\text{P}(1)\text{O}_4$ tetrahedra. These double layers are themselves built from the assemblage of two $[\text{UO}_4(\text{PO}_4)]_\infty$ single layers parallel to (100) (Fig. 1). Each $[\text{UO}_4(\text{PO}_4)]_\infty$ single layer (Fig. 3a) consists of $[\text{UO}_7]_\infty$ chains running along b (resulting from the assemblage of UO_9 polyhedra through an edge) and linked through $\text{P}(2)\text{O}_4$ monophosphate groups. The two single layers that form one double layer are identical, but rotated through 180° about b and shifted by $1/2b + 1/2c$ with respect to each other. They are

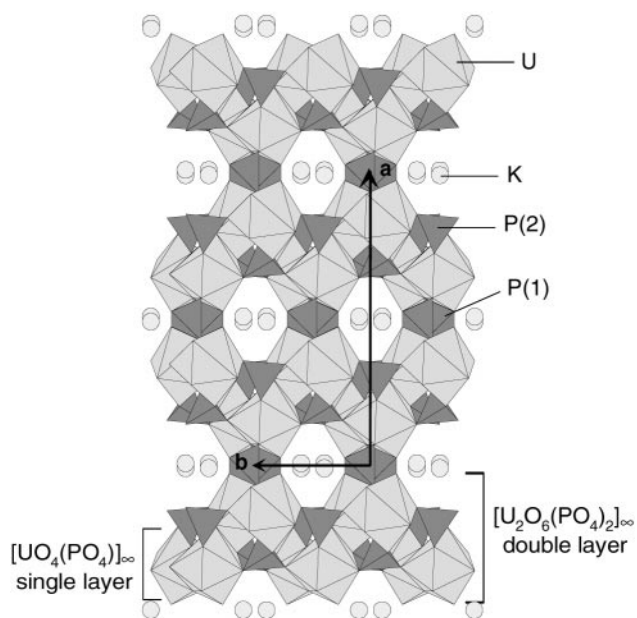


Fig. 1 Projection of the structure of $\text{KU}_2(\text{PO}_4)_3$ along c .

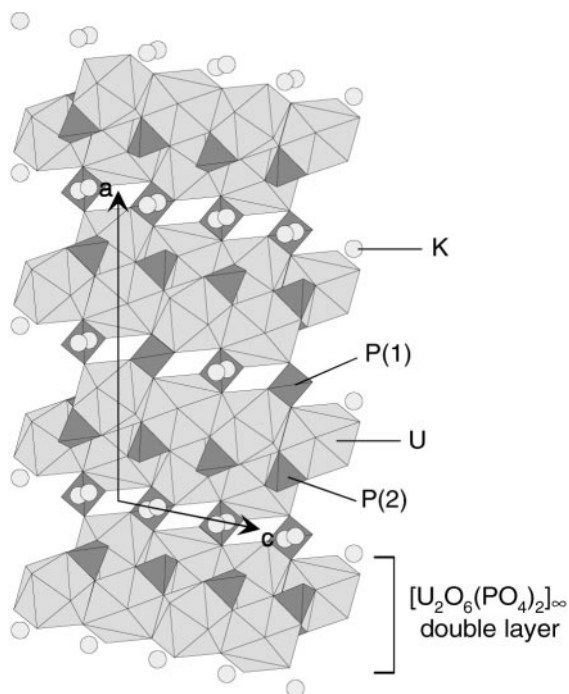


Fig. 2 Projection of the structure of $\text{KU}_2(\text{PO}_4)_3$ along b .

connected in the following way: each UO_9 polyhedron of one layer shares two of its edges with two polyhedra of the second layer, one with another UO_9 polyhedron and the second with a $\text{P}(2)\text{O}_4$ tetrahedron. The projection of the resulting $[\text{U}_2\text{O}_6\{\text{P}(2)\text{O}_4\}_2]_\infty$ double layer is shown in Fig. 3b. It will be noticed that this assemblage gives rise to a bidimensional wavy $[\text{U}_2\text{O}_{12}]_\infty$ network consisting exclusively of UO_9 edge-sharing polyhedra (Fig. 3c).

The junction between the $[\text{U}_2\text{O}_6\{\text{P}(2)\text{O}_4\}_2]_\infty$ double layers is ensured along a via the $\text{P}(1)\text{O}_4$ tetrahedra edge sharing with the UO_9 polyhedra. Since two successive layers are shifted by $1/2b$ with respect to each other (Fig. 1), this assemblage leads to eight-sided tunnels running along c and delimited by four UO_9 polyhedra and four PO_4 tetrahedra, one UO_9 polyhedron alternating with one PO_4 group.

The nine oxygen atoms that surround uranium in this structure form an irregular polyhedron which can be described as intermediate between a trigonal tricapped prism and an Archimedean monocapped antiprism with U–O distances ranging from 2.280(7) to 2.605(7) Å (Table 3). This UO_9 polyhedron is similar to the ThO_9 polyhedra observed in

Table 3 Distances (Å) and angles (°) in $\text{KU}_2(\text{PO}_4)_3$

U–O(1)=2.456(7)		K–O(2)=2.84(1)		
U–O(1i)=2.440(7)		K–O(2vii)=2.78(1)		
U–O(2)=2.454(8)		K–O(3viii)=2.75(1)		
U–O(2i)=2.605(7)		K–O(3)=2.87(1)		
U–O(3)=2.385(7)		K–O(3vii)=3.32(1)		
U–O(4)=2.280(7)		K–O(3ix)=3.03(1)		
U–O(5)=2.502(7)		K–O(4x)=3.21(1)		
U–O(5ii)=2.404(7)		K–O(6)=2.75(1)		
U–O(6)=2.324(8)		K–O(6vii)=2.76(1)		
P(1)	O(2iii)	O(2iv)	O(3ii)	O(3v)
O(2iii)	1.559(7)	2.556(9)	2.58(1)	2.42(1)
O(2iv)	110.1(5)	1.559(7)	2.42(1)	2.58(1)
O(2iii)	113.1(5)	102.7(4)	1.533(8)	2.60(1)
O(3v)	112.7(4)	113.0(4)	115.6(5)	1.533(8)
P(2)	O(1)	O(4iv)	O(5)	O(6vi)
O(1)	1.547(7)	2.549(9)	2.38(1)	2.531(9)
O(4iv)	112.5(4)	1.518(8)	2.509(9)	2.53(1)
O(5)	100.3(4)	109.5(4)	1.555(8)	2.51(1)
O(6vi)	111.4(4)	112.7(4)	109.8(4)	1.517(9)

i: $x; -y; -1/2+z$. ii: $1/2-x; 1/2-y; -z$. iii: $1/2+x; 1/2+y; z$.
 iv: $1/2-x; 1/2+y; 1/2-z$. v: $1/2+x; 1/2-y; 1/2+z$. vi: $1/2-x;$
 $-1/2+y; 1/2-z$. vii: $-x; y; 1/2-z$. viii: $-x; 1-y; -z$.
 ix: $x; 1-y; 1/2+z$. x: $x; -y; -z$.

$\text{KTh}_2(\text{PO}_4)_3$ ¹⁰ and $\text{NaTh}_2(\text{PO}_4)_3$ ¹¹ (note that the thorium environment in $\text{CuTh}_2(\text{PO}_4)_3$ is more irregular, closer to an ‘8+1’ coordination¹⁴).

The monophosphate groups present a classical geometry with four rather homogeneous P–O distances ranging from 1.533(8) to 1.559(7) Å for P(1) and from 1.517(9) to 1.555(8) Å for P(2). Nevertheless, two groups of distances may be distinguished in the P(2) tetrahedron, its two longest P(2)–O bonds corresponding to the O(1)–O(5) edge shared with a UO_9 polyhedron.

The potassium cations sit in the tunnels running along c , split over two half-occupied positions around the two-fold axis. They are surrounded by nine oxygen atoms situated at distances of between 2.75(1) and 3.32(1) Å away (Table 3). Note that splitting of the cationic site was also observed for the sodium atom in the structure of $\text{NaTh}_2(\text{PO}_4)_3$,¹¹ whereas potassium was located on the two-fold axis in $\text{KTh}_2(\text{PO}_4)_3$.¹⁰

An analysis of the electrostatic bond strengths was carried out using the Brese and O’Keeffe relation¹⁷ for K(i), U(iv) and P(v) species with $r_{ij}=2.13, 2.112$ and 1.615, respectively. These

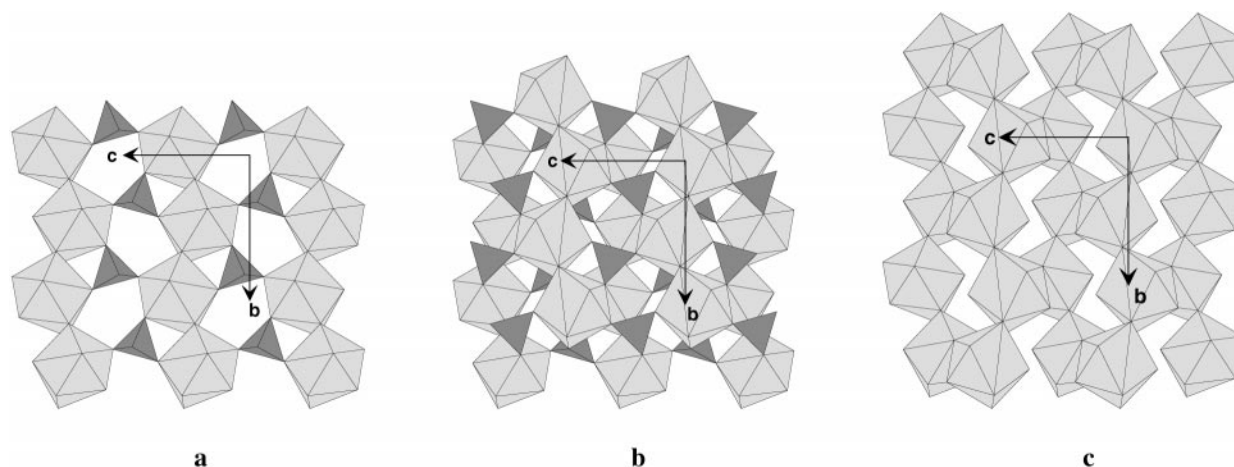


Fig. 3 (a) Projection of a $[\text{UO}_4(\text{PO}_4)]_\infty$ single layer along a . (b) Projection of a $[\text{U}_2\text{O}_6(\text{PO}_4)_2]_\infty$ double layer along a . (c) Projection of a $[\text{U}_2\text{O}_{12}]_\infty$ layer along a .

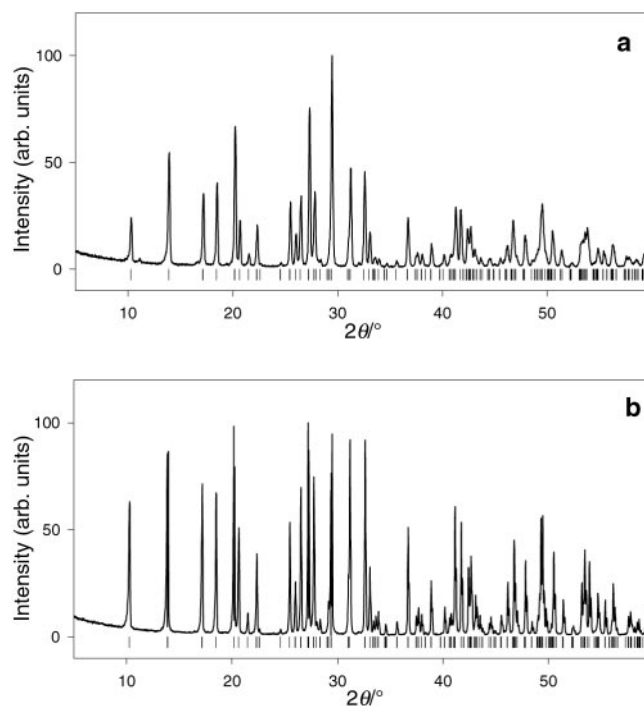


Fig. 4 X-Ray powder diffraction patterns ($\lambda_{\text{Cu-K}\alpha} = 1.5406 \text{ \AA}$). (a) $\text{Ba}_{0.5}\text{Th}_2(\text{PO}_4)_3$, (b) $\text{KTh}_2(\text{PO}_4)_3$.

calculations confirm the tetravalent character of uranium in this compound (calculated value: 3.95).

Cationic non-stoichiometry: $\text{A}_{0.5}\text{Th}_2(\text{PO}_4)_3$ and $\text{K}_{1-2x}\text{Ba}_x\text{Th}_2(\text{PO}_4)_3$ monophosphates

Taking into consideration the above description of the structure, showing that the $[\text{M}_2(\text{PO}_4)_3]_{\infty}$ framework forms tunnels, we have investigated the possibility of cationic non-stoichiometry in the $\text{AM}_2(\text{PO}_4)_3$ structure for $\text{M} = \text{Th}, \text{U}$. All attempts were unsuccessful in the cases of the uranium phosphates, but in contrast to this, a series of new thorium phases isotopic with $\text{KTh}_2(\text{PO}_4)_3$ were isolated. The most remarkable feature is the possibility for complete replacement of the univalent cation by a bivalent cation in this structure. Thus, five new thorium monophosphates of bivalent cations, $\text{A}_{0.5}\text{Th}_2(\text{PO}_4)_3$, have been synthesized for $\text{A} = \text{Cd}, \text{Ca}, \text{Sr}, \text{Pb}, \text{Ba}$. Three of them were obtained in the form of monophasic samples ($\text{A} = \text{Ba}, \text{Sr}, \text{Pb}$), whereas secondary phases appear for $\text{A} = \text{Ca}, \text{Cd}$, corresponding to a mixture of $\text{Th}_4(\text{PO}_4)_4\text{P}_2\text{O}_7^3$ and $\text{CdTh}(\text{PO}_4)_2$ or $\text{CaTh}(\text{PO}_2)_2$ ¹⁸ along with the major phase $\text{A}_{0.5}\text{Th}_2(\text{PO}_4)_3$. The XRPD patterns of these compounds (see Fig. 4a for $\text{A} = \text{Ba}$) are very close to that of $\text{KTh}_2(\text{PO}_4)_3$ (Fig. 4b), and were indexed in a similar monoclinic cell (Table 4). Note that the cell parameters decrease as the size of the interpolated cation decreases from Ba^{2+} to Ca^{2+} . The exception observed for cadmium, whose cell volume is larger than expected, taking into account the smaller size of Cd^{2+} ,

may be due to its ability to form more covalent Cd-O bonds, leading to cadmium sticking to the walls of the tunnels. These results show that large cationic deficiencies may exist in the tunnels (50% of the A sites) without any major distortion of the $[\text{Th}_2(\text{PO}_4)_3]_{\infty}$ framework. Moreover, this non-stoichiometric effect is confirmed by the synthesis of the monophosphate $\text{K}_{1-2x}\text{Ba}_x\text{Th}_2(\text{PO}_4)_3$ with a large homogeneity range, $0 \leq x \leq 0.50$.

Magnetic properties of $\text{KU}_2(\text{PO}_4)_3$ and $\text{KTh}(\text{PO}_4)_3$

The inverse susceptibility curves, $\chi_M^{-1}(T)$ of the two uranium phosphates (Fig. 5) show the paramagnetic behavior of both compounds above 100 K, the modified Curie–Weiss law being obeyed. The calculated magnetic moments, per mole of U, of $3.25 \mu_B$ for $\text{KU}_2(\text{PO}_4)_3$ and $3.14 \mu_B$ for $\text{KTh}(\text{PO}_4)_3$ confirm the tetravalent character of uranium, although they are smaller than the theoretical value ($3.58 \mu_B$). This difference may be due to crystal field effects. Note that below about 50 K the magnetic behavior deviates from the Curie–Weiss law.

Concluding remarks

The possibility to completely substitute uranium for thorium in the $\text{KTh}_2(\text{PO}_4)_3$ phosphate, without any major distortion, has been shown for the first time. But the most important feature deals with the analysis of this framework in terms of a tunnel structure which has allowed a new series of A-site deficient

Table 4 Cell parameters refined from X-ray powder diffraction patterns

Compound	$a/\text{\AA}$	$b/\text{\AA}$	$c/\text{\AA}$	$\beta/^\circ$	$V/\text{\AA}^3$
$\text{KU}_2(\text{PO}_4)_3$	17.4666(4)	6.7519(2)	8.0196(2)	102.035(2)	924.99(4)
$\text{KTh}(\text{PO}_4)_3$	17.560(1)	6.8202(4)	8.0951(5)	101.908(4)	948.6(1)
$\text{KTh}_2(\text{PO}_4)_3$	17.5932(3)	6.8578(1)	8.1355(1)	101.797(1)	960.81(2)
$\text{Ba}_{0.5}\text{Th}_2(\text{PO}_4)_3$	17.5631(6)	6.8614(2)	8.1442(3)	101.562(2)	961.52(6)
$\text{Ba}_{0.4}\text{K}_{0.2}\text{Th}_2(\text{PO}_4)_3$	17.5680(5)	6.8613(2)	8.1454(2)	101.623(2)	961.71(5)
$\text{Ba}_{0.3}\text{K}_{0.4}\text{Th}_2(\text{PO}_4)_3$	17.5673(5)	6.8614(2)	8.1442(2)	101.648(2)	961.45(4)
$\text{Ca}_{0.5}\text{Th}_2(\text{PO}_4)_3$	17.2731(8)	6.8129(3)	8.1391(4)	100.827(3)	940.77(7)
$\text{Cd}_{0.5}\text{Th}_2(\text{PO}_4)_3$	17.4154(7)	6.7909(3)	8.1604(4)	100.377(3)	949.31(7)
$\text{Pb}_{0.5}\text{Th}_2(\text{PO}_4)_3$	17.4572(6)	6.8425(2)	8.1434(3)	101.225(2)	954.13(6)
$\text{Sr}_{0.5}\text{Th}_2(\text{PO}_4)_3$	17.4031(6)	6.8293(2)	8.1480(3)	101.160(2)	950.08(5)

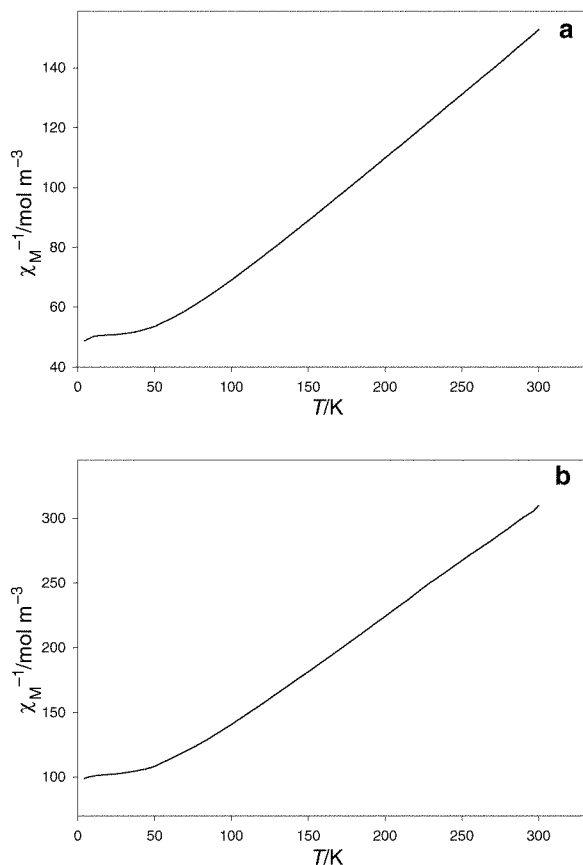


Fig. 5 Inverse molar magnetic susceptibility versus temperature. (a) $\text{KU}_2(\text{PO}_4)_3$, (b) $\text{KTh}(\text{PO}_4)_3$.

isostructural compounds $\text{A}_{0.5}^{\text{II}}\text{Th}_2(\text{PO}_4)_3$ to be synthesized. This non-stoichiometric effect is confirmed by the existence of $\text{K}_{1-2x}\text{Ba}_x\text{Th}_2(\text{PO}_4)_3$ phosphates. These results emphasize the great flexibility of this structure which can be considered as a potential crystalline phosphate matrix for the storage of nuclear waste.

Acknowledgements

We thank Dr D. Pelloquin who kindly performed the electron microscopy study.

References

- 1 G. J. McCarthy, W. B. White and D. E. Pfoertsch, *Mater. Res. Bull.*, 1978, **13**, 1239.
- 2 C. E. Bamberger, R. G. Haire, G. M. Begun and H. E. Hellwege, *J. Less-Common Met.*, 1984, **102**, 179.
- 3 P. Benard, V. Brandel, N. Dacheux, S. Jaulmes, S. Launay, C. Lindecker, M. Genet, D. Louër and M. Quarton, *Chem. Mater.*, 1996, **8**, 181.
- 4 P. Bénard-Rocherullé, M. Louër and D. Louër, *J. Solid State Chem.*, 1997, **132**, 315.
- 5 J. H. Albering and W. Jeitschko, *Z. Kristallogr.*, 1995, **210**, 878.
- 6 Y. Dusausoy, N. E. Ghermani, R. Podor and M. Cuney, *Eur. J. Mineral.*, 1996, **8**, 667.
- 7 V. Brandel, N. Dacheux and M. Genet, *J. Solid State Chem.*, 1996, **121**, 467.
- 8 B. Matkovic and M. Sljukic, *Croat. Chem. Acta*, 1965, **37**, 115.
- 9 B. Matkovic, B. Prodic and M. Sljukic, *Bull. Soc. Chim. Fr.*, 1968, 1777.
- 10 B. Matkovic, B. Prodic and M. Sljukic, *Croat. Chem. Acta*, 1968, **40**, 147.
- 11 B. Matkovic, B. Kojic-Prodic, M. Sljukic, M. Topic, R. D. Willett and F. Pullen, *Inorg. Chim. Acta*, 1970, **4**, 571.
- 12 M. Topic, B. Kojic-Prodic and S. Popovic, *Czech. J. Phys.*, 1970, **B20**, 1003.
- 13 M. Läügt, *J. Appl. Crystallogr.*, 1973, **6**, 299.
- 14 M. Louër, R. Brochu and D. Louër, *Acta Crystallogr., Sect. B*, 1995, **51**, 908.
- 15 J. Rodriguez-Carvajal, in *Satellite Meeting on Powder Diffraction, Abstracts of the XVth Conference of the International Union of Crystallography*, Toulouse, 1990, p. 127.
- 16 S. R. Hall, H. D. Flack and J. M. Stewart, in *XTAL 3.2 Reference Manual*, Universities of Western Australia, Geneva and Maryland, 1992.
- 17 N. E. Brese and M. O'Keeffe, *Acta Crystallogr., Sect. B*, 1991, **47**, 192.
- 18 D. Pfoertsch and G. J. McCarthy, Penn State University, University Park, PA, USA, ICDD Grant-in-Aid, 1978 (PDF no. 31-0311).

Paper 9/04121D